DOI 10.5012/bkcs.2011.32.8.2906

Spontaneous Nanoparticle Formation From a Fluorescent Nucleoside Analogue†

Eun-Kyoung Bang, Dohyun Moon,‡,* and Byeang Hyean Kim*

*Department of Chemistry, Division of IBB, Pohang University of Science and Technology, Pohang 790-784, Korea. *E-mail: bhkim@postech.ac.kr*
*‡Beamline Division, Pohang Accelerator Laboratory, Pohang University of Science and Technology, Pohang 790-784, Korea. *E-mail: dmoon@postech.ac.kr*
Received January 5, 2011, Accepted February 7, 2011

A fluorescent nucleoside analogue, ^{A}**C**, featuring two non-complementary nucleobases linked through an ethynyl group, was synthesized. The extended π-conjugation imparts ^{A}**C** with red-shifted absorbance (relative to adenine and cytosine) and pale-blue fluorescence. It spontaneously forms nanoparticles, which exhibit considerably enhanced fluorescence, without the help of any additional stabilizing agent. The DMSO/water ratio was an important factor influencing the construction of the NPs. X-ray crystallography confirmed the structure of ^{A}**C**; dynamic light scattering and scanning electron microscopy confirmed the existence of the nanoparticles.

Key Words : Nucleosides, Hydrogen bonding, Self-assemblies, Nanoparticles

Introduction

Organic nanoparticles (NPs), which have attracted less attention than their inorganic counterparts, have been investigated mainly in the pharmaceutical industry.[1] Most medicinal compounds have poor solubility in water, but must function under physiological conditions. Studies of various π-conjugated organic dyes, including perylene,[2] pyrazoline,[3] and diarylethene,[4] have revealed that fluorescent organic NPs can exhibit significant changes in fluorescence relative to those of their solvated single molecules. In recent years a diverse range of fluorescent organic NPs (FONs) has been developed for their potential applications in, for example, optoelectronic devices,[5] cancer imaging,[6] biosensors,[7] immunofluorescence labeling,[8] and organic light emitting diodes.[9]

Several nucleoside-based NPs exhibiting increased solubilities in water have been investigated for their pharmaceutical applications. For example, long-alkyl-chain derivatives of acyclovir have been prepared as pro-drugs;[10] these molecules self-assemble, much like liposomes, at the water-air interface, stabilized through hydrophobic interactions and hydrogen bonding. When conjugated with squalene, the nucleoside analogue gemcitabine[11] forms nano-assemblies in water and exhibits increased anticancer activity. Nanoclusters of boron-containing nucleoside conjugates have been studied for their use in anticancer and antiviral therapy.[12] Moreover, some p-conjugated guanosine derivatives modeled on the G-quadruplex have been reported to undergo particle formation.[13]

In this present study, we reported the first case of fluorescent organic nanoparticle formation from a nucleoside analogue without any help of additional fluorogenic molecules or surfactants. The nucleoside analogue ^{A}**C** formed fluorescent nanosize particles and the pale blue fluorescence of ^{A}**C** was significantly enhanced upon its formation of NPs.

Experimental Section

5-(6-Amino-9-ethyl-9*H*-purin-8-yl)ethynyl-2'-deoxycytidine (^{A}C). $(PPh_3)_2PdCl_2$ (67 mg, 0.058 mmol) and CuI (22 mg, 0.12 mmol) were added to a solution of 5-iodo-2'-deoxycytidine (203 mg, 0.58 mmol) and 8-ethynyl-9-ethyladenine (119 mg, 0.64 mmol) in DMF/DIPEA [10:1 (v/v), 6.6 mL]. Argon was bubbled for 2 min through the mixture, which was then subjected to 10 pump/purge cycles before stirring at room temperature for 16 h. After evaporation of the solvent *in vacuo*, the residue was treated with CH_2Cl_2/MeOH (10:1, v/v). The insoluble solid was filtered off and washed sequentially with cold DMF, MeOH, water, acetone, and diethyl ether. The white solid was then dried *in vacuo* (172 mg, 72%). ^{1}H NMR (300 MHz, DMSO-d_6) δ_H = 8.52 (s, 1H), 8.18 (s, 1H), 7.87 (br, 1H), 7.42 (s, 2H), 7. 13 (br, 1H), 6.11 (t, J = 6.15 Hz, 1H), 5.24 (d, J = 4.23 Hz, 1H), 5.13 (t, J = 4.65 Hz, 1H), 4.31-4.21 (m, 1H+2H), 3.83-3.80 (m, 1H), 3.65-3.56 (m, 2H), 2.26-2.18 (m, 1H), 2.11-2.04 (m, 1H), 1.37 (t, J = 7.15 Hz, 3H); ^{13}C NMR (75.5 MHz, DMSO-d_6) δ_C = 163.7, 155.8, 153.6, 153.1, 149.0, 147.1, 133.1, 118.9, 87.6, 87.4, 86.7, 85.8, 83.2, 69.7, 60.7, 41.0, 38.2, 14.9; IR (KBr) ν = 3347, 3206, 2945, 1639, 1601, 1571, 1497, 1377, 1333, 1304, 1257, 1190, 1153, 1094, 1055, 1030 cm^{-1}; mp > 300 °C (ignition); HRMS-FAB (*m/z*): calcd for $C_{18}H_{20}N_8O_4$, 413.1686 $[M + H]^+$.

Crystal data: $C_{42}H_{58}N_{16}O_{11}S_3$; FW = 1059.22 g mol^{-1}; triclinic; space group P1; a = 6.682(1); b = 14.126(3); c = 14.661(3) Å; α = 65.97(3)°; β = 82.42(3)°; γ = 83.79(3)°; V = 1250.6(4) Å^3; T = 100(2) K; Z = 1; $2\theta_{max}$ = 56°; d_{calc} = 1.406 g cm^{-3}; GOF = 1.097; $\mu(\lambda = 0.77000$ Å) = 0.223 mm^{-1}; 8393 reflections were collected; 8393 were unique [R_{int} =

†This paper is dedicated to Professor Eun Lee on the occasion of his honourable retirement.

0.0000]. Refinement of the structure converged at a final R_1 = 0.0460 and wR_2 = 0.1487 for 8393 reflections with $I > 2\sigma(I)$; R_1 = 0.0503, wR_2 = 0.1536 for all reflections. The largest difference peak and hole were 0.475 and −0.675 e Å^{-3}, respectively. Crystal and intensity data are given in Table S1. CCDC-754837 contains the supplementary crystallographic data for this paper. These data can be obtained free of charge via www.ccdc.cam.ac.uk/cgi-bin/catreq.cgi (or from the Cambridge Crystallographic Data Centre, 12, Union Road, Cambridge CB21EZ, UK; fax (+44) 1223-336-033; or deposit @ccdc.cam.ac.uk).

Results and Discussion

We synthesized ^{A}**C** through Sonogashira coupling of adenine and cytidine moieties (Scheme 1) – that is, the hydrogen bonding units that are not complementary. This nucleoside analogue is not soluble in water and other organic solvents such as chloroform, alcohols, and DMF, but soluble in DMSO. During the Sonogashira reaction, we observed that white precipitation of product from the reaction mixture and purified it simply through filtering and repeated washing. Although the hydrogen bonding faces of the adenine and cytidine units in ^{A}**C** cannot interact through Watson-Crick base pairing, electrospray ionization mass spectrometry (ESI-MS) revealed (Figure S1) signals for dimers and trimers of ^{A}**C** in solution (DMSO/methanol/water, 1:4:5).

We obtained a single crystal through vapor diffusion of MeCN into 25 mM ^{A}**C** in DMSO at room temperature; Figure 1 presents the X-ray crystallographic structure. An ORTEP representation of the molecule is displayed in Figure 1(a); Two structures were observed in packing diagram and they feature highly distorted structures, with torsion angles between the planes of the adenine and cytidine nucleobases of 43.97 and 25.19°, respectively (Figures 1(b) and 1(c)). In packing diagram, the molecules interact through a complicated set of hydrogen bonds among the sugar units, nucleobases, and solvent molecules (Figures 1(d) and S2). DMSO molecules are located between the sugar units to bridge pairs of AB layers, each comprising one layer A (Figure S2(a)) and the other layer B (Figure S2(b)), which constructed from the individual structures in Figures 1(b) and 1(c), respectively. Layer A and B interact together through hydrogen bonding and week π-stacking of their hydrophobic nucleobases. To

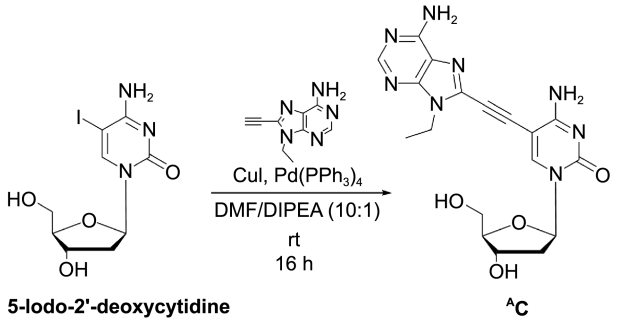

Scheme 1. Synthesis of ^{A}**C**.

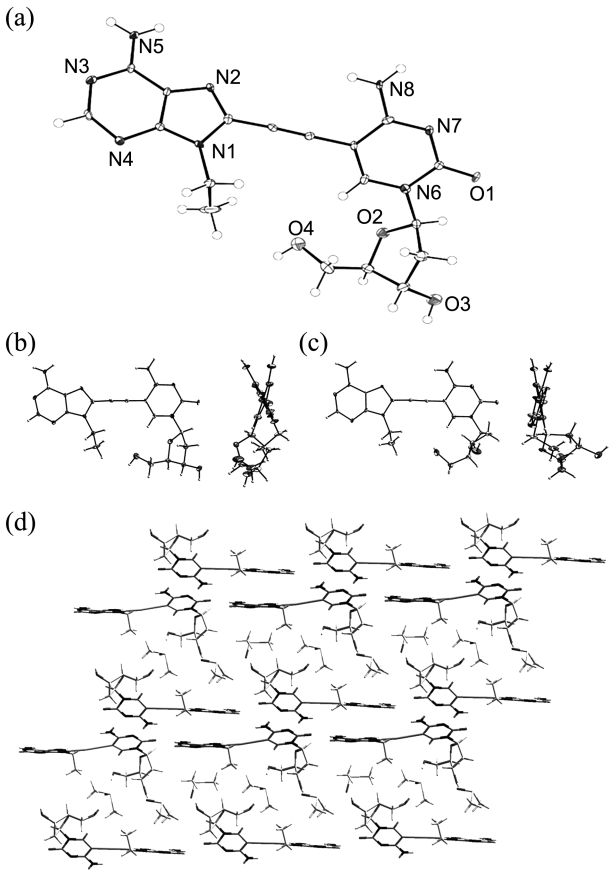

Figure 1. X-ray crystal structure of ^{A}**C** [2($C_{18}H_{20}N_8O_4$)·3(DMSO)] (a) ORTEP plot (50% probability) of ^{A}**C**. (b), (c) Plan and side views of two structures of ^{A}**C** observed in crystal packing structure. (d) Side view of the AB·DMSO·AB·DMSO·A packing lattice of ^{A}**C** layers.

accommodate this complicated series of hydrogen bonds in the solid state, we suspect that the ethynyl linkers in the units of ^{A}**C** underwent rotation to increase their torsion angles from those in solution.

^{A}**C** exhibits pale-blue fluorescence in solution and intense blue fluorescence in the solid state. Because the ethynyl linker provides extended conjugation, the absorption maximum of ^{A}**C** is red-shifted relative to those of adenosine and cytidine themselves. Interestingly, when we diluted the DMSO solution of ^{A}**C** with excess water under vigorous stirring, following the reprecipitation method,[14] we observed highly enhanced fluorescence after 3 days. This phenomenon was caused by the presence of ^{A}**C** NPs; the increase in fluorescence stabilized after 10 days, with no significant change occurring thereafter (even after 6 months). Moreover, this phenomenon was independent on the initial concentration of ^{A}**C** (Figure S3).

Table 1 lists the quantum yields of ^{A}**C**, relative to quinine sulfate (Φ = 0.55),[15] in various states. The quantum yield of ^{A}**C** was just 0.034 in DMSO, and almost zero in water containing 2.5 mol % DMSO directly after preparation. Notably, 30 days later, the quantum yield of the latter solution had increased enormously. Moreover, its emission and excitation maxima had red-shifted by *ca.* 54 and *ca.* 60 nm, respectively.

Table 1. Relative quantum yields (Φ) of **^{A}C** in various environments

System	Φ^{a}	λ_{ex} (nm)	λ_{em} (nm)
^{A}C solution in DMSO	0.034	320	413
^{A}C solution in H_2O/2.5 mol % DMSO[a]	0.004	325	406
^{A}C NPs[b]	0.573	385	460

[a]Measured directly after preparation. [b]Measured 30 days after preparing the solution above.

We recorded the fluorescence spectra of **^{A}C** in water containing 1% DMSO over a period of 10 days at room temperature (Figure 2(a)). The fluorescence of this solution increased over time, reaching 7.0 times the initial intensity after 10 days. As the fluorescence increased, a new absorption band appeared at a wavelength corresponding to that of the excitation maximum at 385 nm (Figure 2(b)); although the absorption maximum remained at 325 nm, the excitation spectrum changed dramatically. The fluorescence intensity when excited at 385 nm was approximately twice that obtained when excited at 325 nm. We suspected that the new absorption band at 385 nm and fluorescence at 460 nm arose from a change in the intramolecular conformation of **^{A}C**.

The formation of **^{A}C** NPs in solution was dependent on the DMSO/water ratio. Increasing the proportion of water caused more NPs to form, but too much water induced the precipitation of **^{A}C**. A lower concentration of **^{A}C** required a lower proportion of DMSO, but some DMSO was necessary in each case to form a transparent solution. When excited at 325 nm, the intensity of the emission band at 460 nm increased and that of the emission band at 406 nm decreased upon increasing the proportion of water (Figure 3(a)). When the NP solutions were excited at 385 nm (excitation maximum), their fluorescence intensity underwent a steep increase upon increasing the proportion of water (Figure 3(b)). A 20 μM solution of **^{A}C** formed NPs (i.e., a recognizable fluorescence change occurred under UV light) when the water content was greater than 95%; a more concentrated, 100 μM solution required only an 80% water content to form NPs (data not shown).

Figure 4(a) displays a photograph of **^{A}C** in solution, in the form of suspended NPs, and in the solid state, with the latter two forms exhibiting intense fluorescence. We detected NPs using dynamic light scattering (DLS) and scanning electron microscopy (SEM). Initially, the particle size was uniform,

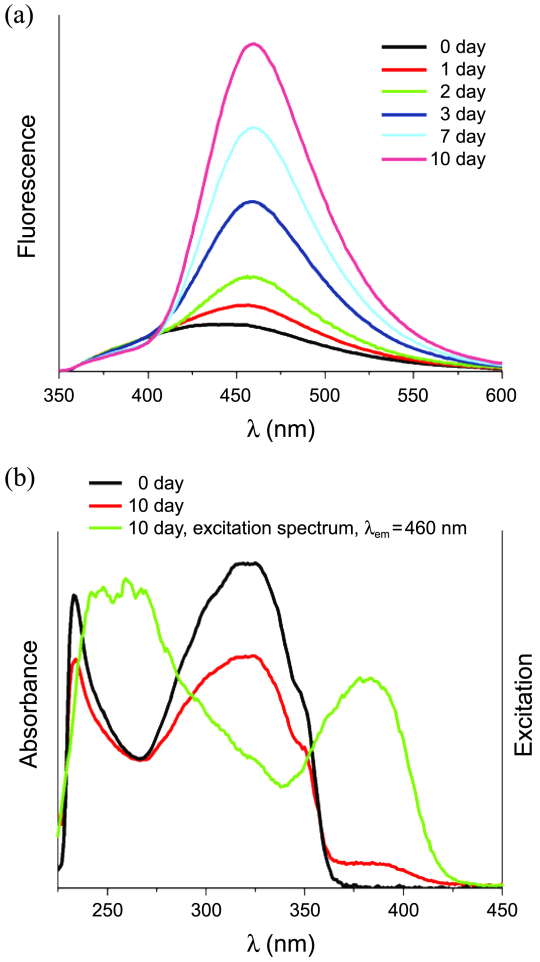

Figure 2. (a) Fluorescence (excitation wavelength: 325 nm) and (b) absorption and excitation (emission wavelength: 460 nm) spectra of **^{A}C** (100 μM in water containing 1% DMSO) recorded over time at 25 °C.

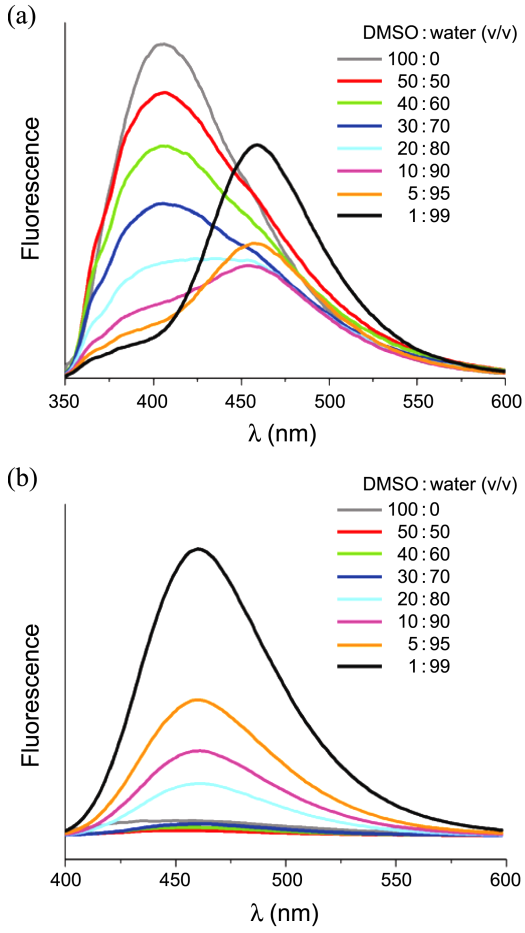

Figure 3. Fluorescence spectra of **^{A}C** (initial concentration: 20 μM) recorded at different DMSO/water ratios, 10 days after preparing each solution. Excitation wavelength: (a) 325 and (b) 385 nm.

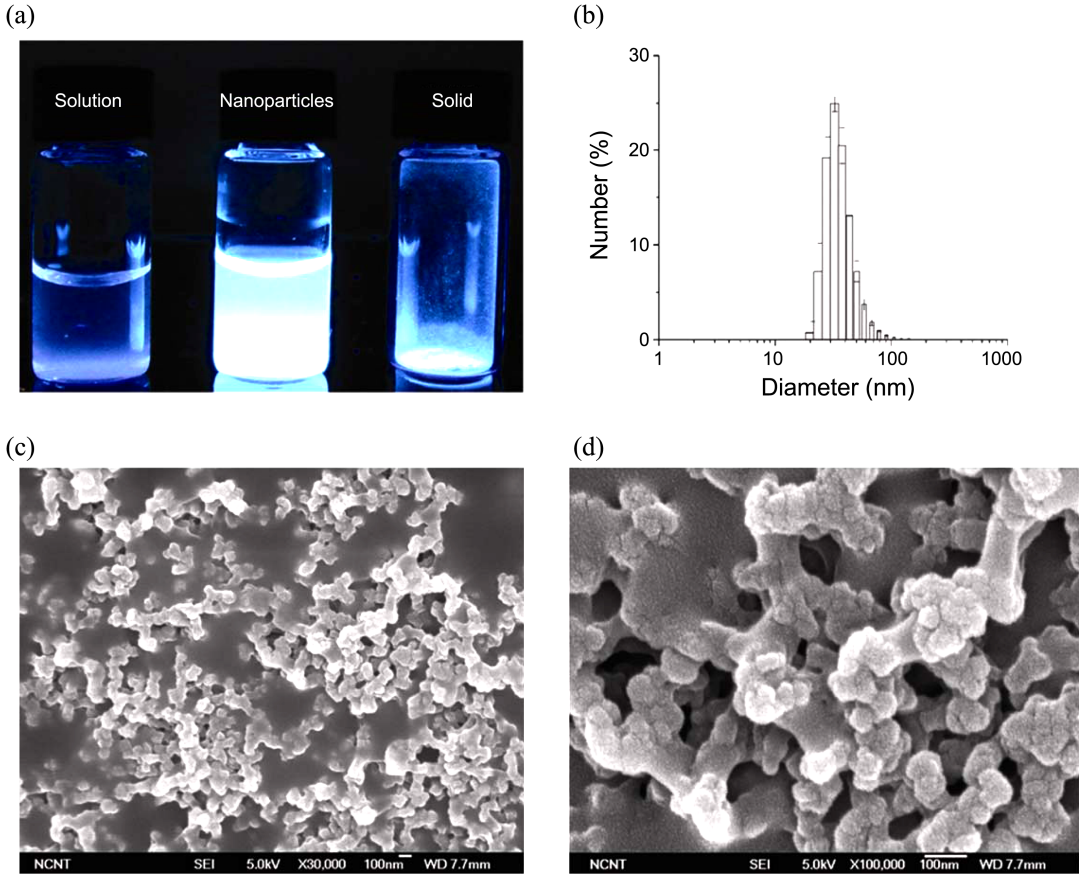

Figure 4. (a) Photograph of three states of ^{A}**C**: in solution, as a suspension of NPs, and as a solid. The solution and NP suspension were prepared in water containing 2.5 mol % DMSO; initial concentration of ^{A}**C**: 100 μM. (b) Distribution of hydrodynamic diameters of NPs, determined using DLS. (c), (d) SEM images of ^{A}**C** NPs, prepared directly on carbon tape.

due to the slow rate of particle formation; over time, however, the NPs aggregated to form irregular larger sized particles (data not shown). Therefore, we determined the hydrodynamic diameters of the NPs after sonication for 1 h, obtaining a mean particle size of 37.7 (± 1.4) nm (Figure 4(b)). SEM imaging supported the existence of aggregates of ^{A}**C** NPs (Figures 4(c) and 4(d)), with individual small NPs clustering together, much like a bunch of grapes.

^{A}**C** spontaneously formed NPs in the absence of any adduct. Once these NPs formed, they exhibited stability toward dilution, changes in pH (from pH 4 to 9), and even heating at 95°C (Figure S4). Indeed, upon increasing the temperature, we observed only weak quenching arising from increased molecular motion and collisions, with the initial fluorescence recovering after cooling to room temperature. Because NP formation at room temperature required more than 10 days, we suspect that the NPs did not dissociate upon heating

Conclusions

We have used Sonogashira coupling to synthesize a fluorescent nucleoside analogue, ^{A}**C**, which features both adenine and cytosine nucleobases. The extended π-conjugation imparts ^{A}**C** with red-shifted absorbance (relative to adenine and cytosine) and pale-blue fluorescence. In the solid state, the adenine and cytosine units were involved in a complicated set of hydrogen bonding and π-stacking interactions. Using a reprecipitation method, ^{A}**C** spontaneously formed NPs without the need for any additional stabilizing agent. ^{A}**C** exhibits strong fluorescence in the solid state and in the form of a suspension of NPs. The excitation and emission maxima of the NPs were red-shifted by ca. 60 nm relative to those of ^{A}**C** in solution. The DMSO/water ratio was an important factor influencing the construction of the NPs. The average size of the initially formed ^{A}**C** NPs was 37.7 (± 1.4) nm, with SEM imaging revealing the presence of clusters of NPs.

Acknowledgments. This study was supported by CRI-Acceleration Research (no. 20100000763) and WCU (R31-10105) programs funded by the Korean government (MEST/NRF). We thank Professor Sungjee Kim for assistance with the DLS measurements and the National Center for Nanomaterials Technology (POSTECH) for the SEM images.

References

1. Horn, D.; Rieger, J. *Angew. Chem. Int. Ed.* **2001**, *40*, 4330.
2. Kasai, H.; Kamatani, H.; Okada, S.; Oikawa, H.; Matsuda, H.; Nakanishi, H. *Jpn. J. Appl. Phys.* **1996**, *34*, L112.

3. Fu, H.-B.; Yao, J.-N. *J. Am. Chem. Soc.* **2001**, *123*, 1434.
4. Sun, F.; Zhang, F.; Zhao, F.; Zhou, X.; Pu, S. *Chem. Phys. Lett.*, **2003**, *380*, 206.
5. (a) An, B.-K.; Kwon, S.-K.; Jung, S.-D.; Park, S. Y. *J. Am. Chem. Soc.* **2002**, *124*, 14410. (b) Lim, S.-J.; An, B.-K.; Jung, S. D.; Chung, M.-A.; Park, S. Y. *Angew. Chem. Int. Ed.* **2004**, *43*, 6346. (c) An, B.-K.; Kwon, S.-K.; Park, S. Y. *Angew. Chem. Int. Ed.* **2007**, *46*, 1978. (d) Kanaparthi, R. K.; Sarkar, M.; Samanta, A. *J. Phys. Chem. B* **2009**, *113*, 15189.
6. Lin, H.-H.; Su, S.-Y.; Chang, C.-C. *Org. Biomol. Chem.* **2009**, *7*, 2036.
7. (a) Li, H.; Yan, H. *J. Phys. Chem.* **2009**, *113*, 7526. (b) Sun, Y.-Y.; Liao, J.-H.; Fang, J.-M.; Chou, P.-T.; Shen, C.-H.; Hsu, C.-W.; Chen, L.-C. *Org. Lett.* **2006**, *8*, 3713.
8. Kim, H.-J.; Lee, J.; Kim, T.-H.; Lee, T. S.; Kim, J. *Adv. Mater.* **2008**, *20*, 1117.
9. Palayangoda, S. S.; Cai, X.; Adhikari, R. M.; Neckers, D. C. *Org. Lett.* **2008**, *10*, 281.
10. Jin, T.; Qiao, Y.; Li, M.; Ai, P.; Hou, X. *Colloid Surface B* **2005**, *42*, 45.
11. (a) Couvreur, P.; Reddy, L. H.; Mangenot, S.; Poupaert, J. H.; Desmaële, D.; Lepêtre-Mouelhi, S.; Pili, B.; Bourgaux, C.; Amenitsch, H.; Ollivon, M. *Small* **2008**, *4*, 247. (b) Bekkara-Aounallah, F.; Gref, R.; Othman, M.; Reddy, L. H.; Pili, B.; Allain, V.; Bourgaux, C.; Hillaireau, H.; Lepêtre-Mouelhi, S.; Desmaële, D.; Nicolas, J.; Chafi, N.; Couvreur, P. *Adv. Funct. Mater*. **2008**, *18*, 3715. (c) Bildstein, L.; Hillaireau, H.; Desmaële, D.; Lepêtre-Mouelhi, S. S.; Dubernet, C.; Couvreur, P. *Int. J. Pharm.* **2009**, *381*, 140.
12. Matějíček, P.; Cígler, P.; Olejniczak, A. B.; Andrysiak, A.; Wojtzak, B.; Procházka, K.; Lensnikowski, Z. J. *Langmuir* **2008**, *24*, 2625.
13. González-Rodríguez, D.; Janssen, P. G. A.; Martín-Rapún, R.; De Cat, I.; De Feyter, S.; Schenning, T. P. H. J.; Meijer, E. W. *J. Am. Chem. Soc.* **2010**, *132*, 4710.
14. Kasai, H.; Nalwa, H. S.; Oikawa, H.; Okada, S.; Matsuda, H.; Minami, N.; Kakuta, A.; Ono, K.; Mukoh, A.; Nakanishi, H. *Jpn. J. Appl. Phys.* **1992**, *31*, L1132.
15. Eaton, D. F. *Pure Appl. Chem.* **1988**, *60*, 110.